Software-Defined Architecture for QoS-Aware IoT Deployments in 5G Systems[☆]

Luis Tello-Oquendo[a,b,d,*], Shih-Chun Lin[c], Ian F. Akyildiz[a], Vicent Pla[b]

[a] *Broadband Wireless Networking Laboratory, School of Electrical and Computer Engineering, Georgia Institute of Technology, Atlanta, GA 30332, USA*
[b] *Instituto ITACA. Universitat Politècnica de València, Valencia 46022, Spain*
[c] *Intelligent Wireless Networking Laboratory, Department of Electrical and Computer Engineering, North Carolina State University, Raleigh, NC 27695, USA*
[d] *College of Engineering, Universidad Nacional de Chimborazo, Riobamba 060108, Ecuador*

Abstract

Internet of Things (IoT), a ubiquitous network of interconnected objects, harvests information from the environments, interacts with the physical world, and uses the existing Internet infrastructure to provide services for information transfer and emerging applications. However, the scalability and Internet access fundamentally challenge the realization of a wide range of IoT applications. Based on recent developments of 5G system architecture, namely SoftAir, this paper introduces a new software-defined platform that enables dynamic and flexible infrastructure for 5G IoT communication. A corresponding sum-rate analysis is also carried out via an optimization approach for efficient data transmissions. First, the SoftAir decouples control plane and data plane for a software-defined wireless architecture and enables effective coordination among remote radio heads (RRHs), equipped with millimeter-wave (mmWave) frontend, for IoT access. Next, by introducing an innovative design of software-defined gateways (SD-GWs) as local IoT controllers in SoftAir, the wide diversity of IoT applications and the heterogeneity of IoT devices are easily accommodated. These SD-GWs aggregate the traffic from heterogeneous IoT devices and

[☆] This work was supported by the US National Science Foundation (NSF) under Grant No. 1547353, in part by the Ministry of Economy and Competitiveness of Spain under Grants TIN2013-47272-C2-1-R and TEC2015-71932-REDT.

[*] Corresponding author
Email address: luis.tello@unach.edu.ec (Luis Tello-Oquendo)

perform protocol conversions between IoT networks and radio access networks. Moreover, a cross-domain optimization framework is proposed in this extended SoftAir architecture concerning both upstream and downstream communication, where the respective sum-rates are maximized and system-level constraints are guaranteed, including (i) quality-of-service requirements of IoT transmissions, (ii) total power limit of mmWave RRHs, and (iii) fronthaul network capacities. Simulation results validate the efficacy of our solutions, where the extended SoftAir solution surpasses existing IoT schemes in spectral efficiency and achieves optimal data rates for next-generation IoT communication.

Keywords: Internet of things (IoT), software-defined networking (SDN), 5G cellular systems, software-defined gateway, millimeter-wave transmissions, cross-domain optimization.

1. Introduction

Internet of Things (IoT) is one of the most transformative and disruptive technologies for the fifth-generation (5G) wireless systems. It has the potential to change the world radically due to its capacity to provide connectivity to anyone/anything at any time and any location. It is anticipated that there will be 20 billion IoT connected devices by 2023 and the global monthly mobile data traffic will achieve 110 exabytes (10^{18} bytes) [1]. However, facing this vast number of IoT devices is a challenging task, in particular, the ubiquitous information transmissions through the backbone networks, such as cellular systems. Moreover, the heterogeneity of IoT devices and the hardware-based, inflexible cellular infrastructure impose even more significant challenges to enable efficient IoT communication.

Current IoT solutions rely on low-power wide area (LPWA) networks, which complement traditional cellular and short-range wireless technologies in addressing IoT applications. Several technologies, such as LoRa, NB-IoT, SIGFOX, have been developed and designed solely for applications with very limited demands on throughput, reliability, or quality-of-service (QoS) [2]. However, with-

out a central regulation among these LPWA technologies, existing IoT solutions cannot support highly diverse QoS requirements from an increasing number of IoT applications. Furthermore, due to currently fixed and hardware-based infrastructure, no existing work has considered the joint architectural design of IoT networks and radio access networks (RANs), and the provision of reliable and efficient upstream/downstream IoT transmissions.

To adequately address the above challenges in 5G IoT, we introduce a new architecture based on the so-called SoftAir [3] to support flexible IoT infrastructure. Also, we propose a sum-rate optimization framework upon SoftAir to yield optimal spectral efficiency in IoT communication. Specifically, inspired by wireless software-defined networking [4, 5], we first propose the SoftAir-based architecture, which decouples control and data planes for an open, programmable, and virtualizable wireless forwarding infrastructure. It allows real time network information accessibility and global optimized control. The data plane consists of software-defined RANs (SD-RANs) and software-defined core networks; the control plane has network management tools and user applications. In SD-RANs, SoftAir centralizes the communication functionality in the baseband server (BBS) pool and enables efficient coordination among hardware-based remote radio heads (RRHs), equipped with millimeter-wave (mmWave) frontend and multiple antennas. Moreover, the cooperativeness of SoftAir facilitates the implementation and aggregation of virtual base stations (VBSs) at the BBS pool to enhance the performance of the system by joint orchestration/optimization [6].

In addition, we propose software-defined gateways (SD-GWs) as local IoT controllers in SoftAir. They can be deployed for satisfying the massive connectivity and diverse traffic generated by a vast number of IoT devices. SD-GWs, serving as the bridge between IoT networks and SD-RANs, provide intensive data aggregation from heterogeneous IoT devices, manage and orchestrate IoT communication, and perform protocol conversions between IoT networks and SD-RANs. This innovative design of SD-GWs enables smooth and ubiquitous information transmissions, traversing between IoT and backbone net-

works. Moreover, upon the SoftAir architecture, we propose a sum-rate optimization framework that maximizes upstream/downstream data rates of IoT communication thus offering low latency and efficient spectrum usage. Based on the physical-layer modeling of mmWave multi-input and multi-output (MIMO) transmissions, the objective is to maximize total data rates from/to SD-GWs through optimal associations of SD-GWs and mmWave RRHs and the respective pre-coding schemes, while guaranteeing (i) QoS requirements from diverse IoT applications, (ii) total power limit of mmWave RRHs, and (iii) fronthaul capacity constraints between the BBS pool and mmWave RRHs.

Our main contributions are summarized as follows:

- A 5G SoftAir-based architecture is introduced to provide efficient, ubiquitous IoT transmissions by supporting a unified software-defined platform for both IoT networks and cellular systems.
- An innovative design of SD-GWs as local IoT controllers is proposed to orchestrate IoT devices and perform protocol conversions between IoT networks and SD-RANs.
- Upon the SoftAir architecture, a sum-rate optimization framework is proposed that achieves efficient spectrum usage and optimal data rates for both upstream and downstream IoT communication.

Simulation results show that our solutions outperform existing IoT infrastructure (with hardware-based architectures and fixed IoT-RAN associations), and achieves optimal rates of 100 Mb/s and 430 Mb/s for upstream and downstream transmissions, respectively. Regarding densely-deployed IoT, we also examine both the impact of increasing the number of mmWave RRHs with a fixed number of antennas and the impact of increasing the number of antennas with a fixed number of mmWave RRHs on the achievable sum-rates. The rest of the paper is organized as follows. Section 2 presents the related work. Section 3 introduces the unified software-defined platform for 5G IoT communication and the system model used in this study. Section 4 proposes the sum-rate analysis

for 5G IoT transmissions via an optimization approach. Section 5 gives the numerical results, and Section 6 concludes the paper.

2. Related Work

While individually, significant research has been carried out in the domains of SDN [7, 8, 9] and IoT [10, 11], a combination of the two remains an open research area and attracts great community attention over the past few years. In [12], SDN is used to enable IoT networks where a central controller translates specific service requirements into network requirements. Both network calculus and a genetic algorithm are respectively adopted to model the multi-network environment and to schedule/route flows, optimizing the end-to-end flow performance. However, the work lacks detailed consideration of network resource sharing in regard to massive IoT devices. In [13], the authors highlight the need to address the heterogeneity of the different IoT devices and applications. They conclude that, although with the introduction of IPv6 the vast increase in the number of connected devices is adequately addressed in part, the heterogeneity among their different requirements and capabilities remains an open research question. To overcome this, a rather high-level architecture of an IoT controller is proposed; at the generic level, it seems an adequate framework to handle heterogeneous IoT flows. However, the work lacks a specific design of the inner workings of the controller and evaluation of the proposed high-level architecture.

Notations: Throughout this paper, boldface lower and upper case symbols represent vectors and matrices, respectively; $\mathbf{I}_x$ denotes the $x \times x$ identity matrix; $\mathbb{C}^{x,y}$ denotes the set of $x \times y$ complex matrices. The trace, transpose, and Hermitian transpose operators are denoted by $\mathrm{tr}(\cdot)$, $(\cdot)^{\mathsf{T}}$, and $(\cdot)^{\mathsf{H}}$, respectively. We use $\mathcal{CN}(\mathbf{X}, \mathbf{Y})$ to denote the circular symmetric complex Gaussian distribution with mean matrix $\mathbf{X}$ and covariance matrix $\mathbf{Y}$; the distribution function of a uniform random variable is denoted by $\mathcal{U}(\cdot)$, the distribution function of a normal random variable with mean x and variance σ^2 is denoted by $\mathcal{N}(x, \sigma)$, and $\sim$ stands for "distributed as". $\|\mathbf{x}\|$ denotes the Euclidean norm of a complex vector $\mathbf{x}$; $|z|$ denotes the magnitude of a complex number z.

In [14], the authors propose a novel SDN-orchestrated network virtualization. There, network slicing is suggested for home network management. Multiple service providers can operate over the same physical infrastructure, each getting an isolated slice of the network, directed by its software controller. What remains somewhat unclear is which algorithms/policies the controller should use, so that the resources are shared amongst the various use-cases. The authors propose the use of a slicing layer that lies between the resource request from the different applications and the network infrastructure substrate. Rather than providing an exact implementation for this layer, the authors only outlined the slicing mechanism. Moving towards the same direction, the authors in [15] argue that the bottleneck in developing vertical, dedicated, application-specific IoT platforms, is the lack of re-usability and interoperability. Instead of each application coming along with its set of sensing hardware, gateways, and cloud computing platform, they propose a horizontal SDN-based IoT platform. The architecture is divided into four layers: a device layer (sensing devices and the actuators); a communication layer (SDN-enabled switches and gateways); a computing layer (SDN controller(s) and the accounting/billing functions), and a service layer (used by the IoT application developers to give high-level instructions to the controller, which in turn will translate them to specific network commands). However, [15] does not provide for integration of the sensing devices with the proposed platform (i.e., the SDN controller does not interact with the sensing domain), so their behavior is not defined by the SDN controller.

Having IoT applications in mind, in [16] a general SDN-IoT framework based on the classic SDN architecture is defined. It consists of a service layer, a network layer, and a sensing layer, composed of IoT end-devices. In the upper layer, servers provide the developers with the necessary APIs for IoT applications; in the middle layer, the distributed network operative system (OS) is contained, commanding several physically distributed SDN controllers; and in the lower layer, the SDN-enabled network switches with an IoT gateway (to connect them to the middle layer) are contained. Virtualization techniques are used to design the network OS with the aim of achieving an IoT-optimized network. This

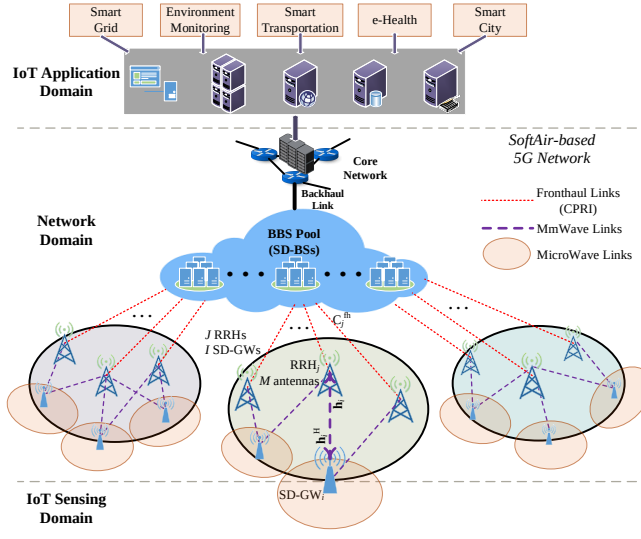

Figure 1: Unified software-defined platform for 5G IoT communication.

network OS must be used in such a way that the diversity of use-cases and IoT devices is acknowledged. However, integration of the proposed SDN and NFV for an IoT-optimized network has not been implemented, and specific details about how virtualization is going to be used in the middle layer are missing.

3. Uniform software-defined platform for 5G IoT communication

Extended from our preliminary study in [3], Fig. 1 shows the proposed 5G SoftAir architecture that supports a flexible IoT infrastructure and seamless device connectivity. Specifically, it consists of three domains: sensing, network, and application. Besides, a security and privacy sublayer is considered that is transversal to all the domains and protects the availability, integrity, and privacy for all connected resources and information when things will be deployed on the large scale.

The *sensing domain* enables IoT devices to interact and communicate with each other, through the data collection technologies such as wireless sensor networks, RFID, ZigBee or near-field communication. The *network domain* builds

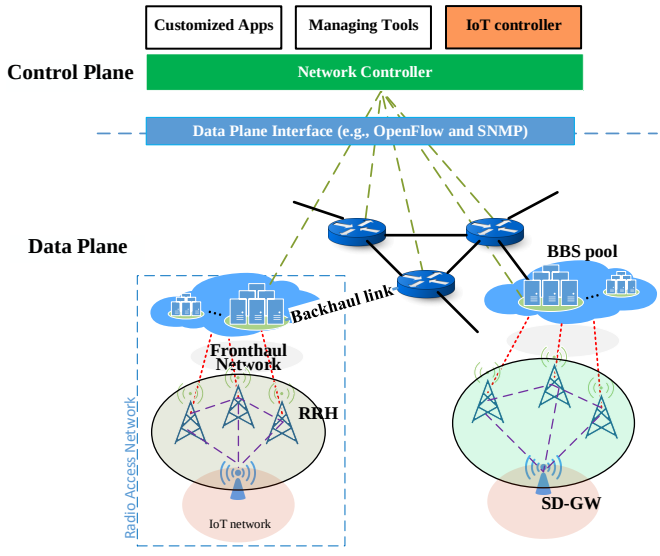

Figure 2: A SoftAir architecture for IoT communication within 5G systems.

on SoftAir; it consists of three parts as depicted in Fig. 2: (i) the centralized BBS pool, which connects to the core network via backhaul links; it has software-defined BSs (SD-BSs) from real-time virtualization technology that allow for software-implemented baseband units (e.g., digital processing tasks), (ii) mmWave RRHs plus antennas, which are remotely controlled by SD-BSs and serve SD-GWs' transmissions, and (iii) low-latency high-bandwidth fronthaul links (fiber or microwave) using the common public radio interface (CPRI) for an accurate, high-resolution synchronization among mmWave RRHs. The objective of this network domain is to transfer the data collected from the sensing domain to the remote destination. Finally, the *application domain* is responsible for data processing and the provision of a wide variety of applications and services.

Regarding the security and privacy sublayer, transversal to all the domains, it is set to protect the communications throughout the entire system and to ensure all trusted devices/data will be operated/processed. Concretely, an identity-based networking service is proposed that use flow rules to control

the traffic arrivals through security devices. The IEEE 802.1X protocol can be implemented for switch-port based network access control, jointly with the lightweight directory access protocol (LDAP) for authentication along with an access control server that implements radius, AAA authentication, and network access control lists (flow rules to control traffic in and out). Furthermore, this sublayer also implements secure shell (SSH), HTTPS, and IPSEC tunneling for remote access and monitoring.

Additionally, the controller architecture deploys several virtualized components such as task-resource matching, service specification, and flow scheduling to address the heterogeneous and dynamic needs of IoT applications and services. The *task-resource matching* component maps the task request of IoT applications or services onto the existing resources in IoT heterogeneous networks. The *service solution specification* component maps the features of devices and services involved in the communication to precise requirements for devices, networks, and application constraints. The *flow scheduling* component schedules the flows that satisfy the specified requirements. Note that the heterogeneity of the networks and various QoS requirements of flows becomes the scheduling and coordination of the resources in IoT networks complex. Preprocessing and analysis will be performed at the edge of the networks if necessary through *fog computing*. Finally, we use a logically centralized management and coordination component for addressing the synchronization and inter-controller communications. By doing so, our proposed architecture will orchestrate the end-to-end communication and the necessary resources for satisfying the IoT connectivity with strict QoS requirements and energy constraints.

It is worth noting that an essential architectural component is the SD-GW, that lies between the sensing and network domain. Besides alleviating high traffic loads from tremendously heterogeneous IoT devices, these SD-GWs aggregate the data from randomly deployed IoT devices and provide Internet access to IoT networks through SD-RANs. SD-GWs also manage IoT connectivity and orchestrate IoT devices by regulating parameters in network protocols. Therefore, they can receive IoT data traffic from the IoT sensing devices and forward

the traffic to the SoftAir SD-RAN. Depending on the communication direction, each SD-GW will either perform protocol conversions in such a way it can forward the data to the SoftAir system with the maximum achievable rate or forward the data to the IoT devices meeting the application QoS requirements. In [17], we considered the joint architectural design of IoT networks and software-defined radio access networks (SD-RANs) to the provision of reliable and efficient upstream/downstream IoT transmissions.

3.1. System Model

The system model of SoftAir consists of a set $\mathcal{I} = \{1, \ldots, I\}$ of SD-GWs that are served by a set $\mathcal{J} = \{1, \ldots, J\}$ of associated RRHs. All RRHs are connected to the BBS pool $\mathcal{B}$ via fronthaul links, where the jth fronthaul link between the $j \in \mathcal{J}$ RRH and the $\mathcal{B}$ BBS pool has a predetermined capacity $C_j^{(\mathrm{fh})}$. The BBS pool performs most baseband processing tasks while transmission functions are realized by the RRHs using the processed baseband signals received from the BBS through the fronthaul transport network. The associations between the SD-GWs and RRHs can be determined based on the distance or channel gain from each RRH to each SD-GW. These RRHs are equipped with an array of M antennas and communicate with the single-antenna SD-GWs through mmWave links. Note that by using low-latency high-bandwidth fronthaul links, the software-defined architecture implements an accurate, high-resolution synchronization and enables flexible coordination among RRHs. One RRH can serve a group of SD-GWs: when the jth RRH is assigned to serve the ith SD-GW, this RRH receives the SD-GW's processed baseband signal from the BBS pool and then modifies the pre-coding vectors accordingly.

4. Sum-Rate Analysis for 5G IoT Communication via an Optimization Approach

In the following, we first model the peculiarities of mmWave transmissions in the SoftAir architecture; then, we propose a protocol for mmWave RRH

discovery and association; finally, we develop a sum-rate optimization framework that jointly optimizes RRHs' beamforming weights and associations between RRHs and SD-GWs for maximum upstream/downstream spectral efficiency, while guaranteeing QoS and system-level constraints.

4.1. Millimeter-Wave Communication

We introduce the link budget for the ith mmWave communication link between the ith SD-GW and jth RRH. Particularly, we detail the path-loss l_i, channel vector $\mathbf{h}_i$, and beamforming gain $G_i^{(\mathrm{BF})}$ to derive the achievable upstream rate $R_i^{(\mathrm{ul})}$ and downstream rate $R_i^{(\mathrm{dl})}$, respectively.

4.1.1. Path-Loss

Considering the special characteristics of mmWave propagation (such as short-range communication, inevitable blockage effects, and sparse-scattering radio patterns), the path-loss for a mmWave communication link l_i can be modeled with three link-states: outage (l_{iO}), LoS (l_{iL}) or NLoS (l_{iN}) [18]. These three states are formulated as follows

$$l_{iO} = 0; \quad l_{iL} = (\alpha_L d_i)^{-\beta_L}; l_{iN} = (\alpha_N d_i)^{-\beta_N}, \tag{1}$$

where α_L (α_N) can be interpreted as the path-loss of the LoS (NLoS) link at 1 [m] distance, and β_L (β_N) denotes the path-loss exponent of the LoS (NLoS) link; from experimental results [18], β_N value (can be up to 4) is normally higher than β_L value (i.e., 2). Then, each link-state is formulated by the probabilities $\mathbb{P}_O$, $\mathbb{P}_L$, and $\mathbb{P}_N$, respectively, as

$$\begin{aligned} \mathbb{P}_O &= \max(0, 1 - \gamma_O e^{-\delta_O d_i}); \\ \mathbb{P}_L &= (1 - \mathbb{P}_O)\gamma_L e^{-\delta_L d_i}; \\ \mathbb{P}_N &= (1 - \mathbb{P}_O)(1 - \gamma_L e^{-\delta_L d_i}), \end{aligned} \tag{2}$$

where d_i denotes the transmitter-receiver distance; the parameters γ_L (γ_O) and δ_L (δ_O) depend on both the propagation scenario and the considered carrier frequency [19].

Table 1: Three-state Link Path Loss Model Computation Parameters and the Occurrence Probabilities of LOS, NLOS, and Outage States at 73 [GHz] from Experimental Data in [18, 19]

Path loss model (three-state link)	$\alpha_L = 10^{\frac{69.8}{20}}$, $\beta_L = 2$
Eqs. (1)-(3)	$\alpha_N = 10^{\frac{82.7}{26.9}}$, $\beta_N = 2.69$
Path loss model (three-state link) and log-normal shadowing Eqs. (1)-(3)	$\alpha_L = 10^{\frac{69.8+\zeta_L}{20}}$, $\beta_L = 2$ $\zeta_L\,[dB] \sim \mathcal{N}(0, 5.8^2)$ $\alpha_N = 10^{\frac{82.7+\zeta_N}{26.9}}$, $\beta_N = 2.69$ $\zeta_N\,[dB] \sim \mathcal{N}(0, 7.7^2)$
LOS-NLOS-outage probability parameters Eq. (2)	$\gamma_L = 1, \delta_L = 1/67.1$ $\gamma_O = \exp(5.2), \delta_O = 1/30$

Thus, the corresponding path-loss component of the channel is modeled as

$$\begin{aligned} l_i = &\mathbb{I}[U < \mathbb{P}_L(d_i)] l_{iL} + \\ &\mathbb{I}[\mathbb{P}_L(d_i) \leq U < (\mathbb{P}_L(d_i) + \mathbb{P}_N(d_i))] l_{iN} + \\ &\mathbb{I}[(\mathbb{P}_L(d_i) + \mathbb{P}_N(d_i)) \leq U \leq 1] l_{iO}, \end{aligned} \tag{3}$$

where $\mathbb{I}[x]$ is the indicator function, it returns 1 when x is true, and 0 otherwise; $U \sim \mathcal{U}[0, 1]$ is a uniform random variable. For computing the path-loss model, we use the parameter values at 73 GHz as shown in Table 1.

4.1.2. Channel Vector

Besides the peculiarities of mmWave transmissions [18, 20], the blockage information is not entirely feasible; therefore, we exploit the stochastic geometry analysis for modeling the mmWave channel vector [20]. Specifically, we model the channel vector as $\mathbf{h}_i = \sqrt{l_i \boldsymbol{\beta}_i}\, \boldsymbol{\xi}_i \in \mathbb{C}^{M,1}$, where l_i is the large-scale path-loss in power of the mmWave communication link i (which might also include log-normal shadowing), $\boldsymbol{\beta}_i \in \mathbb{C}^{M,M}$ is the co-variance matrix for antenna correlations in small-scale fading, and $\boldsymbol{\xi}_i \in \mathbb{C}^{M,1}$ is a Gaussian vector with the zero-mean circularly symmetric Gaussian noise distribution $\mathcal{CN}(0, \mathbf{I}_M)$ for the fast-fading.

4.1.3. Beamforming

To ensure an acceptable range of the communication in the multi-antenna mmWave transmissions, we introduce the precode vectors, i.e., beamforming weights at the RRHs, where the weight vector $\mathbf{w}_i \in \mathbb{C}^{M,1}$ is the linear downlink beamforming vector at the jth RRH corresponding to the ith SD-GW. The beamforming gain is given as $G_i^{(\mathrm{BF})} = \mathbf{w}_i^{\mathsf{H}} \boldsymbol{\beta}_i \mathbf{w}_i$, with $\boldsymbol{\beta}_i$ being the covariance matrix of the channel response vector $\mathbf{h}_i$. In the case where the fading is fully correlated between the antennas, the matched filtering pre-coding method is exploited as $\boldsymbol{\beta}_i = \mathbf{h}_i^{\mathsf{H}} \mathbf{h}_i$ and $\mathbf{w}_i = \mathbf{h}_i / \|\mathbf{h}_i\|$; therefore, $G_i^{(\mathrm{BF})} = \|\mathbf{h}_i\|^2$.

4.2. Protocol for MmWave RRH Discovery

We consider a time-division duplex (TDD) mode to exploit channel reciprocity in uplink and downlink transmissions; it offers availability of timely and accurate feedback of channel state information (CSI). Also, in SoftAir the VBSs in the central BBU pool can easily share CSI associated with different users in the system.

Specifically, the time-frequency wireless resources are divided into frames, where a frame consists of T_f seconds and W Hz and leaves room of $S = T_f\, W$ transmission symbols, as shown in Fig. 3. In each frame, $D \geq 1$ out of the S symbols are dedicated for allocating the RRH's reference signal (RS); the remaining $S - D$ symbols are used for payload data where $1 - \kappa$ and κ denote the fixed fractions for uplink and downlink transmissions, respectively.

Each RRH broadcasts its RS at the beginning of every frame. The RS is of duration $T_{rs} \ll T_f$. In each frame i, a mmWave RRH transmits the RS using beamformer $\mathbf{w}_i$. Each RRH needs I consecutive frames to complete one cycle of spatial scanning using I beamformers [21]. At the receiving end, each SD-GW collect signal from $\digamma$ frames and performs non-coherent detection to detect the presence of RSs and their timings. The parameter $\digamma$ can be set to $\digamma = K\, I$, where $K \geq 1$ is an integer. By doing so, we ensure that, in presence of spatial scanning, each SD-GW has been covered by at least one beam and can accumulate sufficient energy for detection purposes.

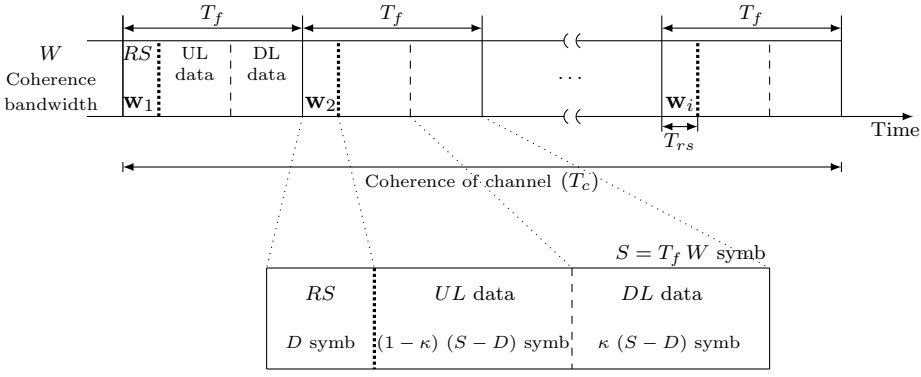

Figure 3: Frame structure with beamforming transmission of RS in TDD mode.

4.2.1. Association Scheme

Let $\mathcal{J} = \{1, \ldots, J\}$ and $\mathcal{I} = \{1, \ldots, I\}$ denote the set of RRHs and SD-GWs in the SoftAir system, respectively. Suppose that each SD-GW is served by a specific group (cluster) of associated RRHs, and a RRH can serve multiple SD-GWs at the same time. To express the association status between RRHs and SD-GWs, we introduce the following binary variables as the indicators. Concretely, RRHs can be active to serve SD-GWs or shutdown to save the energy consumption, let $\{q_j, j \in \mathcal{J}\}$ denotes the activity of RRHs as

$$q_j = \begin{cases} 1, & \text{the } j\text{th RRH is in active mode;} \\ 0, & \text{otherwise;} \end{cases} \tag{4}$$

let $\{g_{ij}, i \in \mathcal{I}, j \in \mathcal{J}\}$ denotes the association between RRHs and SD-GW as

$$g_{ij} = \begin{cases} 1, & \text{the } i\text{th SD-GW is served by the } j\text{th RRH;} \\ 0, & \text{otherwise;} \end{cases} \tag{5}$$

furthermore, to characterize the group (cluster) of serving RRHs, let $\{N_{ij}, i \in \mathcal{I}, j \in \mathcal{J}\}$ be the clustering indicator as

$$N_{ij} = \mathbb{I}[j \in \mathcal{N}_i], \tag{6}$$

where $\mathcal{N}_i$ denotes the set of near RRHs for the ith SD-GW which can be determined based on the distance or channel gain from RRHs to each SD-GW.

4.3. Achievable Sum-Rate Analysis

In the following, we first investigate channel estimation; then, we study the ergodic achievable spectral efficiency and capacity in both, the upstream and downstream IoT communication.

4.3.1. Minimum mean-square error (MMSE) Channel Estimation

During a training phase in TDD networks, the SD-GWs served by a cluster $\mathcal{N}_i$ of RRHs transmit mutually orthogonal pilot sequences which allow the BBS pool to compute the estimate $\hat{\mathbf{H}}_i$ of the local channel $\mathbf{H}_i$. While the same set of orthogonal pilot sequences might be reused among RRH clusters, the channel estimate is corrupted by pilot contamination from adjacent clusters [22]. After correlating the received training signals $\breve{\mathbf{Y}}_i$ with the pilot sequences $\mathbf{w}_i$, the BBS pool acquires the noisy observation as

$$\breve{\mathbf{Y}}_i^* = \breve{\mathbf{Y}}_i \mathbf{w}_i^{\mathsf{H}} \triangleq [\breve{\mathbf{y}}_1^* \cdots \breve{\mathbf{y}}_I^*] \in \mathbb{C}^{M|\mathcal{N}_i|,I}, \tag{7}$$

and accordingly estimates the channel vector $\mathbf{h}_i$. Specifically, we adopt the MMSE estimator [23] which gives the estimate $\hat{\mathbf{h}}_i$ of $\mathbf{h}_i$ as

$$\begin{aligned} \hat{\mathbf{h}}_i &= \mathbf{A}_i \mathbf{Q}_i \breve{\mathbf{y}}_i^* \\ &= \mathbf{A}_i \mathbf{Q}_i \left(\mathbf{h}_i + \sum_{k \in \mathcal{N}} \mathbf{h}_k + \frac{1}{\sqrt{\rho_{tr}}} \breve{\mathbf{n}}_i \right) \sim \mathcal{CN}\left(\mathbf{0}, \mathbf{\Phi}_i\right), \end{aligned} \tag{8}$$

where

$\mathbf{A}_i \quad \triangleq \mathbb{E}[\mathbf{h}_i \, \mathbf{h}_i^{\mathsf{H}}] \in \mathbb{C}^{M|\mathcal{N}_i|, M|\mathcal{N}_i|}$;

$\mathbf{Q}_i \quad = \left(\frac{1}{\rho_{tr}} \mathbf{I}_{M|\mathcal{N}_i|} + \sum_{k \in \mathcal{J}} \mathbf{A}_k \right)^{-1}$;

$\sqrt{\rho_{tr}}$ denotes the effective training signal-to-noise (SNR) ratio, $\rho_{tr} > 0$;

$\breve{\mathbf{n}}_i \quad \sim \mathcal{CN}\left(\mathbf{0}, \mathbf{I}_{M|\mathcal{N}_i|}\right)$;

$\mathcal{N}$ denotes the set of other clusters that use the same pilot as the one adopted in cluster $\mathcal{N}_i$ for the SD-GW i;

$\mathbf{\Phi}_i \quad = \mathbf{A}_i \mathbf{Q}_i \mathbf{A}_k, k \in \mathcal{J}$.

Applying the orthogonality of the MMSE estimate, the channel vector can be further decomposed as $\mathbf{h}_i = \hat{\mathbf{h}}_i + \tilde{\mathbf{h}}_i$, where $\tilde{\mathbf{h}}_i \sim \mathcal{CN}(\mathbf{0}, \mathbf{A}_i - \mathbf{\Phi}_i)$ is the uncorrelated (and also statistically independent) estimation error [24, 22].

4.3.2. Upstream Transmissions (IoT Networks to SD-RANs)

Following the above multi-antenna mmWave transmission characterization over a link i, the received base-band signal vector $\mathbf{y} \in \mathbb{C}^{M,1}$ at the BBS at a given instant reads $\mathbf{y}^{(\mathrm{ul})} = \sqrt{P^{(\mathrm{ul})}}\mathbf{H}\mathbf{x}^{(\mathrm{ul})} + \eta^{(\mathrm{ul})}$, where each element of the received signal vector corresponds to a BBS antenna, $\mathbf{H} = [\mathbf{h}_1 \cdots \mathbf{h}_I] \in \mathbb{C}^{M,I}$, $\mathbf{h}_i \in \mathbb{C}^{M,1}$ denotes the mmWave channel corresponding to the ith SD-GW, $\mathbf{x}^{(\mathrm{ul})} = [x_1 \cdots x_I]^{\mathsf{T}}$ denotes the I×1 vector containing the transmitted signals from all the SD-GWs, $P^{(\mathrm{ul})}$ is the average transmit power of each SD-GW, and $\eta^{(\mathrm{ul})} \sim \mathcal{CN}(0, \sigma)$ is the zero-mean circularly symmetric Gaussian noise with noise power σ^2.

The BBS processes the received signal vector and obtains the estimated channel matrix by multiplying the Hermitian-transpose of the MMSE detection matrix with the signal at the receiver as $\tilde{\mathbf{y}}^{(\mathrm{ul})} = \hat{\mathbf{H}}^{\mathsf{H}}\mathbf{y}^{(\mathrm{ul})} = \hat{\mathbf{H}}^{\mathsf{H}}\mathbf{H}\mathbf{x}^{(\mathrm{ul})} + \hat{\mathbf{H}}^{\mathsf{H}}\eta^{(\mathrm{ul})}$. The ith element of $\tilde{\mathbf{y}}^{(\mathrm{ul})}$ can be written as $\tilde{y}_i^{(\mathrm{ul})} = \sqrt{P_i^{(\mathrm{ul})}}\hat{\mathbf{h}}_i^{\mathsf{H}}\mathbf{H}\mathbf{x}^{(\mathrm{ul})} + \hat{\mathbf{h}}_i^{\mathsf{H}}\eta^{(\mathrm{ul})}$, where $\mathbf{h}_i$ is the ith column of $\mathbf{H}$. By the elements multiplication, we further get $\tilde{y}_j^{(\mathrm{ul})} = \sqrt{P_i^{(\mathrm{ul})}}\hat{\mathbf{h}}_i^{\mathsf{H}}\mathbf{h}_i x_i + \sum_{k=1,k\neq i}^{I}\sqrt{P_k^{(\mathrm{ul})}}\hat{\mathbf{h}}_i^{\mathsf{H}}\mathbf{h}_i x_k + \hat{\mathbf{h}}_i^{\mathsf{H}}\eta^{(\mathrm{ul})}$, where x_i denotes the ith element of $\mathbf{x}^{(\mathrm{ul})}$. Then, the signal-to-interference-plus-noise ratio (SINR) achieved by the ith SD-GW, $\gamma_i^{(\mathrm{ul})}$, is

$$\gamma_i^{(\mathrm{ul})} = P_i^{(\mathrm{ul})}|\hat{\mathbf{h}}_i^{\mathsf{H}}\mathbf{h}_i|^2 / (\textstyle\sum_{k=1,k\neq i}^{I} P_k^{(\mathrm{ul})}|\hat{\mathbf{h}}_i^{\mathsf{H}}\mathbf{h}_k|^2 + \|\hat{\mathbf{h}}_i\|^2\sigma^2). \tag{9}$$

Assuming an ergodic channel [25], the achievable uplink rate of the ith SD-GW is given by

$$R_i^{(\mathrm{ul})} = B\log_2(1 + \gamma_i^{(\mathrm{ul})}), \tag{10}$$

where B denotes the wireless transmission bandwidth. We define the uplink sum rate [bits/s/Hz] per cell considering the associations between RRHs and SD-GWs as follows

$$C^{(\mathrm{ul})} = \sum_{j\in\mathcal{J}}\sum_{i\in\mathcal{I}} g_{ij}N_{ij}R_i^{(\mathrm{ul})}. \tag{11}$$

4.3.3. Downstream Transmissions (SD-RANs to IoT Networks)

The received base band signal $y^{(\mathrm{dl})} \in \mathbb{C}$ at the ith SD-GW is given as $y^{(\mathrm{dl})} = \sqrt{P_j^{(\mathrm{dl})}}\mathbf{h}_i^{\mathsf{H}}\,\mathbf{s} + \eta^{(\mathrm{dl})}$, where $\mathbf{s} \in \mathbb{C}^{M,1}$ is the signal vector intended for the ith SD-GW with $P_j^{(\mathrm{dl})}$ average power; $\eta^{(\mathrm{dl})} \sim \mathcal{CN}(0, \sigma^2)$ is the receiver noise. We assume channel reciprocity, i.e., the downlink channel $\mathbf{h}_i^{\mathsf{H}}$ is the Hermitian transpose of the uplink channel $\mathbf{h}_i$. The transmit vector $\mathbf{s}$ is given as $\mathbf{s} = \sqrt{\upsilon}\sum_{i=1}^{I}\mathbf{w}_i x_i = \sqrt{\upsilon}\,\mathbf{W}\,\mathbf{x}^{(\mathrm{dl})}$, where $\mathbf{W} = [\mathbf{w}_1 \cdots \mathbf{w}_I] \in \mathbb{C}^{M,I}$ is a precoding matrix (i.e. the network beamforming design) and $\mathbf{x}^{(\mathrm{dl})} = [x_1 \cdots x_I]^{\mathsf{T}} \in \mathbb{C}^{I,1}$ contains the data symbols for the ith SD-GW. The parameter υ normalizes the average transmit power per RRH to $\mathbb{E}[\frac{P_j^{(\mathrm{dl})}}{I}\mathbf{s}^{\mathsf{H}}\,\mathbf{s}] = P_j^{(\mathrm{dl})}$, i.e., $\upsilon = \left(\mathbb{E}\left[\frac{1}{I}\mathrm{tr}(\mathbf{W}\,\mathbf{W}^{\mathsf{H}})\right]\right)^{-1}$. We consider a linear precoder of practical interest, namely eigenbeamforming, which can be defined as $\mathbf{w}_i = \hat{\mathbf{h}}_i$ for $i \in \mathcal{I}$.

The associated SINR achieved by the ith SD-GW, $\gamma_i^{(\mathrm{dl})}$, is

$$\gamma_i^{(\mathrm{dl})} = \upsilon \left|\mathbb{E}\left[\mathbf{h}_i^{\mathsf{H}}\hat{\mathbf{h}}_i\right]\right|^2 / \left(\sum_{k=1,k\neq i}^{I} \upsilon\,\mathbb{E}\left[|\mathbf{h}_i^{\mathsf{H}}\hat{\mathbf{h}}_k|^2\right] + \sigma^2\right). \tag{12}$$

Since the SD-GWs do not have any channel estimate, we provide an ergodic achievable rate based on the techniques developed in [25, Theorem 1]. Hence, by assuming that the average effective channels $\sqrt{\upsilon}\left|\mathbb{E}\left[\mathbf{h}_i^{\mathsf{H}}\hat{\mathbf{h}}_i\right]\right|^2$ can be perfectly learned by the SD-GW, the ergodic achievable spectral efficiency at SD-GW i of RRH cluster $\mathcal{N}_i$ is given as

$$R_i^{(\mathrm{dl})} = B_i(1-\kappa)\log_2(1+\gamma_i^{(\mathrm{dl})}), \tag{13}$$

where B_i is the bandwidth allocated to the ith SD-GW, κ accounts for the spectral efficiency loss due to signaling at RRH.

The downlink sum rate [bits/s/Hz] per cell considering the associations between RRHs and SD-GWs is

$$C^{(\mathrm{dl})} = \sum_{j\in\mathcal{J}}\sum_{i\in\mathcal{I}} g_{ij}N_{ij}R_i^{(\mathrm{dl})}. \tag{14}$$

4.4. SD-GWs' QoS Requirements and Optimization Framework

Besides supporting almost pervasive device connectivity, IoT applications demand services with different rate requirements; therefore, we formulate those

requirements in terms of SINR coverage and achieved sum-rate per cell at the SD-RAN. We optimize associations between RRHs and SD-GWs so that the SD-GW sum-rate is maximized, and the QoS requirements of SD-GWs and system-level constraints are satisfied simultaneously.

Given ϑ as the minimum tolerable SINR over a link i, the SINR constraints of SD-GWs can be formulated as

$$\gamma_i \geq \vartheta, \forall i \in \mathcal{I}, \tag{15}$$

where γ_i is computed by either (9) or (12) in case of uplink or downlink transmission, respectively. From the association scheme, we can obtain the equality $q_j = 1 - \prod_{i=1}^{I} (1 - g_{ij} N_{ij}), \forall j \in \mathcal{J}$ and the following sets of association constraints between RRHs and SD-GW:

$$q_j \geq g_{ij} N_{ij}, \forall i \in \mathcal{I}, j \in \mathcal{J}; \tag{16}$$

$$\textstyle\sum_{j=1}^{J} g_{ij} N_{ij} \geq 1, \forall i \in \mathcal{I}, \tag{17}$$

where (16) implies that a RRH is in active mode if it is associated with at least one SD-GW whereas (17) ensures that each SD-GW is served by at least one RRH. On the other hand, given the pre-coding vector at the jth RRH for the ith SD-GW, the transmitter power used by this RRH to serve the ith SD-GW is $\mathbf{w}_i^{\mathsf{H}} \mathbf{w}_i$ [26]. Let $P_j^{(\text{r-max})}$ denote the maximum power of the jth RRH, we impose the constraints on RRHs' downlink beamforming weights as follows

$$\textstyle\sum_{i=1}^{I} \mathbf{w}_i^{\mathsf{H}} \mathbf{w}_i \leq q_j P_j^{(\text{r-max})}, \forall j \in \mathcal{J}; \tag{18}$$

$$\mathbf{w}_i^{\mathsf{H}} \mathbf{w}_i \leq g_{ij} N_{ij} P_j^{(\text{r-max})}, \forall i \in \mathcal{I}, j \in \mathcal{J}, \tag{19}$$

where (18) limits the total transmit power of each RRH and (19) ensures that the transmit power from the jth RRH to the ith SD-GW is set to zero if there is no association between them. Furthermore, by only allowing the links in $\mathcal{N}_i$ (see Section 4.2.1) we set the beamforming weights of mmWave communication links as

$$\mathbf{w}_i^{\mathsf{H}} \mathbf{w}_i = 0 \text{ if } N_{ij} = 0, \forall i \in \mathcal{I}, j \in \mathcal{J}, \tag{20}$$

so that we reduce all possible links between the J RRHs and the I SD-GWs to $|\mathcal{N}_i|$ links (typically $|\mathcal{N}_i| \ll JI$), which in turns dramatically shrinks the size of the possible solution sets of precoding vectors for lower computation complexity[27, 26]. Additionally, the per-fronthaul capacity constraints (neglecting the fronthaul capacity consumption for transferring compressed beamforming vector) are formulated as follows

$$C \leq C^{(\mathrm{fh})}, \tag{21}$$

where C is computed by (11) in uplink transmission or by (14) in downlink transmission. This indicates that the total data rate transmitted at the each RRH should be less or equal to the rate forwarded by the fronthaul link.

We aim at maximizing the total achievable uplink/downlink data rates at SD-GWs; the overall optimization framework for the SD-RAN becomes

$$\begin{aligned} \text{Find} \quad & q_j \in \{0,1\}, g_{ij} \in \{0,1\}, P_i^{(\mathrm{ul})}, P_j^{(\mathrm{dl})}, \mathbf{w}_i, \\ & \forall i \in \mathcal{I}, j \in \mathcal{J} \\ \text{maximize} \quad & C = \textstyle\sum_{i=1}^{I} R_i, \\ \text{subject to} \quad & (15), (16), (17), (18), (19), (20), (21), \end{aligned} \tag{22}$$

where R_i is calculated based on the communication direction: upstream [see (10)], downstream [see (13)]. The decision variables take values from a discrete set that leads the optimization framework to an integer programming problem. The size of this problem allows the controller to yield a solution in few seconds through exhaustive searching methods. The acquired solutions are then processed by both the BBS pool and the SD-GW for optimal upstream/downstream transmissions.

5. Numerical Results

In this section, we present the simulation results of our proposed designs in Section 4.4. In all experiments, each evaluation point represents the average value of 10^4 samples considering the dynamic update of associations in

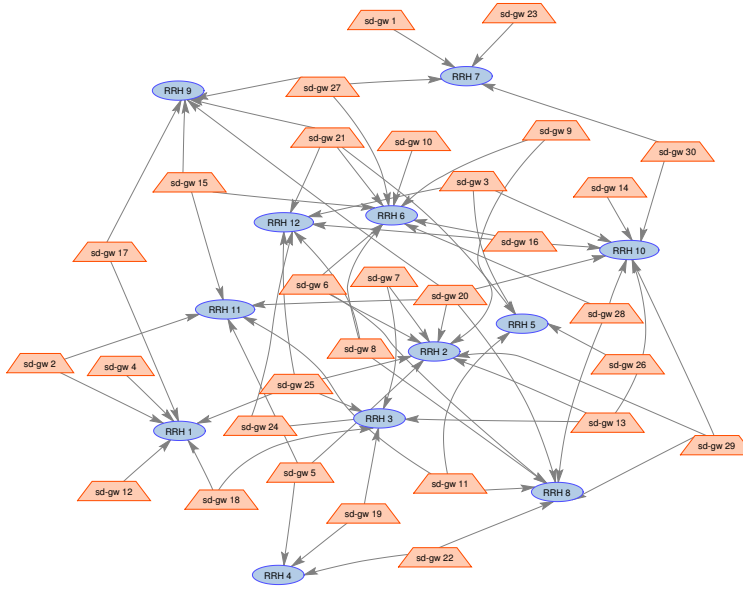

Figure 4: Example of the network topology and association establishment: 12 RRHs that serve 30 SD-GWs deployed in such an area.

the deployed infrastructure. We examine both the spectral efficiency and the achievable rate per SD-GW in SoftAir. Towards this, we have a set $\mathcal{J}$ of $J = 12$ RRHs, each one equipped with $M = 4$ antennas; the coverage area of every RRH has a radius of 200 [m]. They serve several SD-GW densities ranging from 30 to 100 SD-GWs randomly distributed in the coverage area of RRHs. Fig. 4 illustrates an example of the network topology and the associations established between RRHs and SD-GWs based on the protocol proposed in Section 4.2.

The wireless bandwidth is set as $B = 500$ [MHz], and the carrier frequency is set as 73 [GHz]. The channel vectors are generated according to the mmWave communication modeling in Section 4.1, where the three-state path-loss model with log-normal shadowing is considered. The transmit power constraint for each RRH is $P_j^{(\text{r-max})} = 45$ [dBm]. The maximum transmission power of each SD-GW is set as 23 [dBm] and the thermal noise power is assumed to be -101 [dBm/Hz]. Moreover, we assume that all RRHs possess the same fronthaul capacity, i.e., $C_j^{(\text{fh})} = 6$ [bits/s/Hz], $\forall j \in \mathcal{J}$. As 64 QAM is set as the highest

constellation supported in the system, the maximum spectrum efficiency per data stream is 6 [bits/s/Hz].

We first analyze the spectral efficiency and compare the performance of our proposed designs with that of the following benchmark associations [19] for existing IoT communication: (i) highest received power association, (ii) smallest path-loss association. In the former, each SD-GW will be served by the RRH providing the highest received power to it based on uplink or downlink RSs which undergo both path-loss and shadowing. In the latter, an SD-GW will be served by the RRH with the smallest path-loss to it. This association comes to the fact that user equipments might be unable to consider random fluctuations by shadowing because the pronounced blockage impact on received signals produces less slowly-varying shadowing in mmWave transmissions.

Fig. 5 shows that the spectral efficiency of our SoftAir design is on average 24% higher in uplink transmission as depicted in Fig. 5a and 11% higher in downlink transmission where it peaks at 12.6 b/s/Hz with 40 SD-GWs deployed, then slightly declines as the number of SD-GWs increases as depicted in Fig. 5b. Regarding achievable sum-rate per SD-GW, Fig. 6 depicts the uplink and downlink rate as a function of the deployed SD-GWs. The data rate achieved by our solution is up to 50% higher than that of conventional solutions. Note that as the number of served SD-GWs increases, both uplink and downlink rate per SD-GW decrease due to more significant interference.

We further consider densely deployed IoT scenarios and explore the impact of increasing either the number of RRHs or the number of antennas at each RRH on the achievable sum-rates. On the one hand, Fig. 7 illustrates that increasing the number of RRHs significantly improves the achievable uplink rate at SD-GWs whereas the achievable downlink rate experiences small changes. On the other hand, Fig. 8 indicates the increasing number of antennas at RRHs dramatically improves the achievable downlink rate at SD-GWs whereas the achievable uplink rate remained almost steady. In particular, the network hereby has 12 associated RRHs with 4 antennas; each RRH serves 80 randomly deployed SD-GWs in the coverage area of the RRHs. These results show that there is a trade-off between

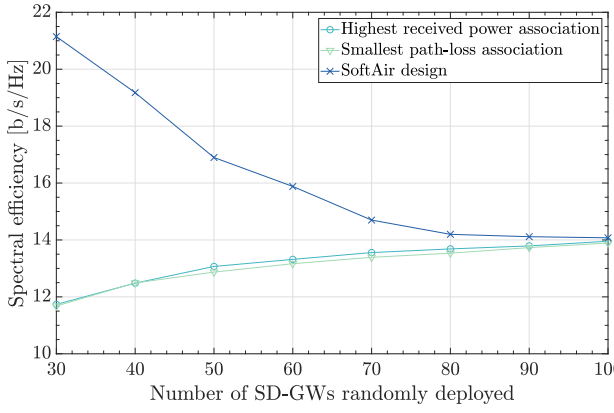

(a)

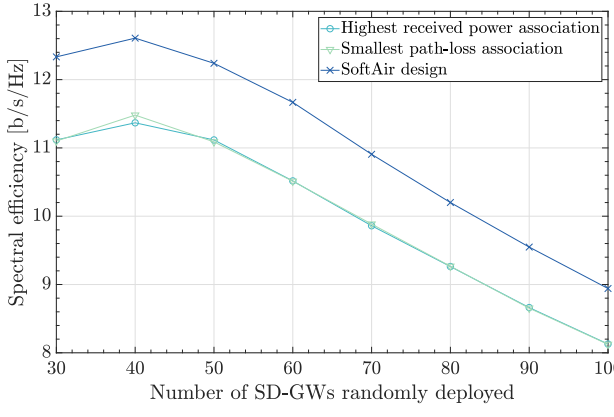

(b)

Figure 5: Spectral Efficiency [b/s/Hz]; 12 RRHs deployed to serve different densities of SD-GWs; carrier frequency: 73 GHz. (a) Upstream IoT transmissions. (b) Downstream IoT transmissions.

increasing the number of RRHs and increasing the number of antennas at RRHs that affects the achievable rate depending on the direction of the transmission.

To sum up, our SoftAir solution provides ultrahigh data rates (i.e., 430 Mb/s rate in downlink and 100 Mb/s rate in uplink through mmWave transmissions) for each SD-GW in densely deployed scenarios, and a decision for increasing the number of RRHs or the number of antennas at RRHs can be made according to the IoT applications.

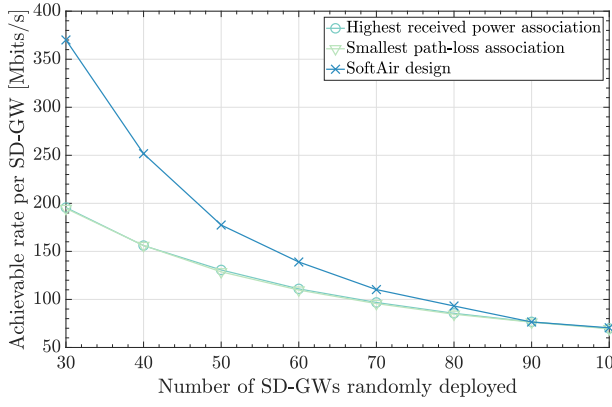

(a)

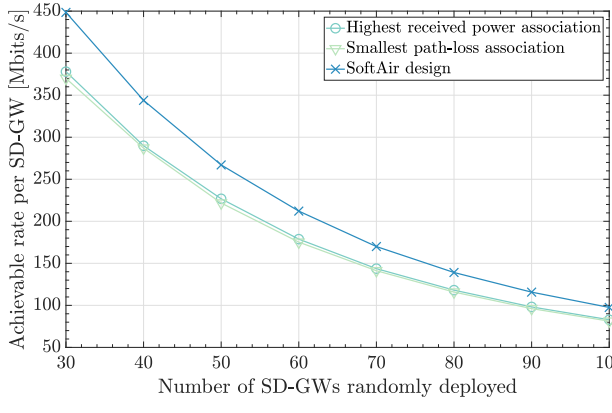

(b)

Figure 6: Achievable rate for the SoftAir design and two existing IoT solutions with conventional mmWave schemes. (a) Upstream IoT transmissions. (b) Downstream IoT transmissions.

6. Conclusion

In this paper, we introduced a 5G SoftAir architecture and provided optimal sum-rates for both upstream and downstream IoT communication. First, by jointly exploiting mmWave frontend, MIMO, and virtualization, the SoftAir system is adopted which gives software-defined infrastructure and enables effective coordination among mmWave RRHs. Then, SD-GWs are designed in SoftAir as local controllers that manage and orchestrate IoT transmissions between IoT

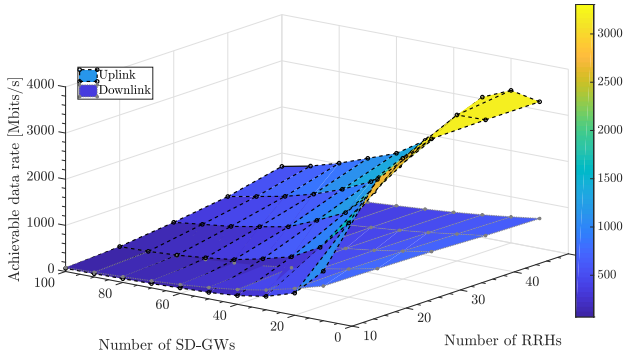

Figure 7: Impact of increasing the number of RRHs on the achievable uplink/downlink rates; the SD-GWs randomly deployed ranges from 10 to 100, and the number of RRHs ranges from 10 to 50.

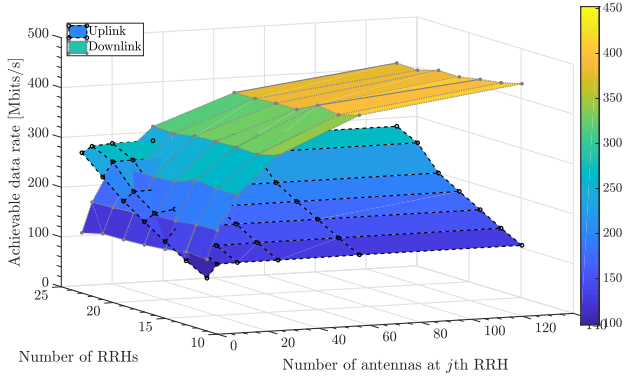

Figure 8: Impact of increasing the number of RRHs or/and antennas at RRHs on the achievable uplink/downlink rates; 80 SD-GWs randomly deployed that are served by a set of RRHs.

networks and SD-RANs. Moreover, a sum-rate optimization framework is proposed in the extended SoftAir, where total data rates of upstream/downstream IoT communication is maximized through optimal associations between mmWave RRHs and SD-GWs. Simulation results validate the superiority of our solutions than conventional IoT schemes, where the extended SoftAir solution achieves optimal spectral efficiency for 5G IoT communication.

References

[1] Ericsson, Ericsson mobility report (Nov. 2017).
URL https://www.ericsson.com/mobility-report

[2] U. Raza, P. Kulkarni, M. Sooriyabandara, Low power wide area networks: An overview, IEEE Commun. Surveys Tuts. PP (99).

[3] I. F. Akyildiz, P. Wang, S.-C. Lin, SoftAir: A software defined networking architecture for 5G wireless systems, Computer Networks 85 (2015) 1 – 18. doi:http://dx.doi.org/10.1016/j.comnet.2015.05.007.

[4] I. F. Akyildiz, S.-C. Lin, P. Wang, Wireless software-defined networks (W-SDNs) and network function virtualization (NFV) for 5G cellular systems: An overview and qualitative evaluation, Computer Networks 93, Part 1 (2015) 66 – 79. doi:http://dx.doi.org/10.1016/j.comnet.2015.10.013.

[5] I. F. Akyildiz, S. Nie, S.-C. Lin, M. Chandrasekaran, 5G roadmap: 10 key enabling technologies, Computer Networks 106 (2016) 17 – 48. doi:http://dx.doi.org/10.1016/j.comnet.2016.06.010.

[6] A. Gran, S. Lin, I. F. Akyildiz, Towards wireless infrastructure-as-a-service (WlaaS) for 5G software-defined cellular systems, in: 2017 IEEE International Conference on Communications (ICC), 2017, pp. 1–6. doi:10.1109/ICC.2017.7996597.

[7] N. Feamster, J. Rexford, E. Zegura, The road to SDN, Queue 11 (12) (2013) 20.

[8] A. Lara, A. Kolasani, B. Ramamurthy, Network innovation using openflow: A survey, IEEE Commun. Surveys Tuts. 16 (1) (2014) 493–512.

[9] B. A. A. Nunes, M. Mendonca, X.-N. Nguyen, K. Obraczka, T. Turletti, A survey of software-defined networking: Past, present, and future of programmable networks, IEEE Commun. Surveys Tuts. 16 (3) (2014) 1617–1634.

[10] A. Al-Fuqaha, M. Guizani, M. Mohammadi, M. Aledhari, M. Ayyash, Internet of things: A survey on enabling technologies, protocols, and applications, IEEE Communications Surveys & Tutorials 17 (4) (2015) 2347–2376.

[11] M. Noura, M. Atiquzzaman, M. Gaedke, Interoperability in internet of things: Taxonomies and open challenges, Mobile Networks and Applicationsdoi:10.1007/s11036-018-1089-9.
URL https://doi.org/10.1007/s11036-018-1089-9

[12] Z. Qin, G. Denker, C. Giannelli, P. Bellavista, N. Venkatasubramanian, A software defined networking architecture for the Internet-of-Things, in: Network Operations and Management Symposium (NOMS), 2014 IEEE, IEEE, 2014, pp. 1–9.

[13] Y. Jararweh, M. Al-Ayyoub, E. Benkhelifa, M. Vouk, A. Rindos, et al., SDIoT: a software defined based Internet of Things framework, Journal of Ambient Intelligence and Humanized Computing 6 (4) (2015) 453–461.

[14] Y. Yiakoumis, K.-K. Yap, S. Katti, G. Parulkar, N. McKeown, Slicing home networks, in: Proceedings of the 2nd ACM SIGCOMM workshop on Home networks, ACM, 2011, pp. 1–6.

[15] Y. Li, X. Su, J. Riekki, T. Kanter, R. Rahmani, A SDN-based architecture for horizontal Internet of Things services, in: Communications (ICC), 2016 IEEE International Conference on, IEEE, 2016, pp. 1–7.

[16] J. Li, E. Altman, C. Touati, A general SDN-based IoT framework with NVF implementation, ZTE communications 13 (3) (2015) 42–45.

[17] L. Tello-Oquendo, I. F. Akyildiz, S. Lin, V. Pla, SDN-based architecture for providing reliable Internet of Things connectivity in 5G systems, in: 2018 17th Annual Mediterranean Ad Hoc Networking Workshop (Med-Hoc-Net), 2018, pp. 1–8. doi:10.23919/MedHocNet.2018.8407080.

[18] M. R. Akdeniz, Y. Liu, M. K. Samimi, S. Sun, S. Rangan, T. S. Rappaport, E. Erkip, Millimeter wave channel modeling and cellular capac-

ity evaluation, IEEE J. Sel. Areas Commun. 32 (6) (2014) 1164–1179. doi:10.1109/JSAC.2014.2328154.

[19] M. D. Renzo, Stochastic geometry modeling and analysis of multi-tier millimeter wave cellular networks, IEEE Trans. Wireless Commun. 14 (9) (2015) 5038–5057. doi:10.1109/TWC.2015.2431689.

[20] T. Bai, R. W. Heath, Asymptotic SINR for millimeter wave massive MIMO cellular networks, in: 2015 IEEE 16th International Workshop on Signal Processing Advances in Wireless Communications (SPAWC), 2015, pp. 620–624. doi:10.1109/SPAWC.2015.7227112.

[21] C. Liu, M. Li, I. B. Collings, S. V. Hanly, P. Whiting, et al., Design and analysis of transmit beamforming for millimeter wave base station discovery., IEEE Trans. Wireless Communications 16 (2) (2017) 797–811.

[22] J. Hoydis, S. Ten Brink, M. Debbah, Massive mimo in the ul/dl of cellular networks: How many antennas do we need?, IEEE J. Sel. Areas Commun. 31 (2) (2013) 160–171.

[23] S. M. Kay, Fundamentals of statistical signal processing, volume i: Estimation theory (v. 1), PTR Prentice-Hall, Englewood Cliffs.

[24] S.-C. Lin, H. Narasimhan, Towards software-defined massive mimo for 5g&b spectral-efficient networks, in: 2018 IEEE International Conference on Communications (ICC), IEEE, 2018, pp. 1–6.

[25] J. Jose, A. Ashikhmin, T. L. Marzetta, S. Vishwanath, Pilot contamination and precoding in multi-cell TDD systems, IEEE Trans. Wireless Commun. 10 (8) (2011) 2640–2651. doi:10.1109/TWC.2011.060711.101155.

[26] V. N. Ha, L. B. Le, N. D. Dao, Coordinated multipoint transmission design for cloud-rans with limited fronthaul capacity constraints, IEEE Trans. Veh. Technol. 65 (9) (2016) 7432–7447. doi:10.1109/TVT.2015.2485668.

[27] S.-C. Lin, I. F. Akyildiz, Dynamic base station formation for solving NLOS problem in 5G millimeter-wave communication, in: IEEE Conference on Computer Commun. (INFOCOM), 2017, pp. 1–9. doi:10.1109/INFOCOM.2017.8057227.